Inter-correlated gut microbiota and SCFAs changes upon antibiotics exposure links with rapid body-mass gain in weaned piglet model

Che, Lianqiang; Hu, Qi; Wang, Ru; Zhang, Du; Liu, Cong; Zhang, Yihe; Xin, Guizhong; Fang, Zhengfeng; Lin, Yan; Xu, Shengyu; Feng, Bin; Chen, Daiwen; Wu, De; Gao, Fei

Published in:
Journal of Nutritional Biochemistry

DOI:
10.1016/j.jnutbio.2019.108246

Publication date:
2019

Document version
Publisher's PDF, also known as Version of record

Available online at www.sciencedirect.com

ScienceDirect

Journal of Nutritional Biochemistry 74 (2019) 108246

Journal of Nutritional Biochemistry

Inter-correlated gut microbiota and SCFAs changes upon antibiotics exposure links with rapid body-mass gain in weaned piglet model

Lianqiang Che[a,*,1], Qi Hu[b,1], Ru Wang[a], Du Zhang[b], Cong Liu[b], Yihe Zhang[b], Guizhong Xin[d], Zhengfeng Fang[a], Yan Lin[a], Shengyu Xu[a], Bin Feng[a], Daiwen Chen[a], De Wu[a], Fei Gao[b,c,**]

[a]Animal Nutrition Institute, Sichuan Agricultural University, Ya'an, China
[b]Genome Analysis Laboratory of the Ministry of Agriculture, Agricultural Genomics Institute at Shenzhen, Chinese Academy of Agricultural Sciences, Shenzhen, China
[c]Comparative Pediatrics and Nutrition, Department of Veterinary and Animal Sciences, Faculty of Health and Medical Sciences, University of Copenhagen, Frederiksberg, DK, Denmark
[d]State Key Laboratory of Natural Medicines, Department of Chinese Medicines Analysis, China Pharmaceutical University, Nanjing, China

Received 18 April 2019; received in revised form 18 July 2019; accepted 10 September 2019

Abstract

The risk of overweight or obesity in association with early exposure of antibiotics remains an important public issue for health-care of children. Low-dose antibiotics (LDA) have been widely used to enhance growth rate of pigs, providing a good animal model to study the underlying mechanism. In present study, 28 female piglets, weaned at 21 d, were randomly classified into two groups, receiving either a control diet or a diet supplemented with LDA for 4 weeks. The total bacterial load and intestinal microbiota were determined by qPCR and 16S rRNA amplicon sequencing. UPLC-QTRAP-MS/MS and RNA-seq were further used to determine the colonic SCFAs and transcriptomes. Results showed that LDA significantly increased growth rate and food intake. The F/B index, *Methanosphaera species*, and the pathway of "carbohydrate metabolism" were improved by LDA exposure, indicating the better carbohydrate degradation and energy utilization. Furthermore, correlation analysis indicated the microbial community contributing to SCFAs production was enriched upon LDA exposure, associating with increased concentrations of short-chain and branched-chain fatty acids (caproate, 2-methyl butyrate and 4-methyl valerate). A multivariate linear fitting model analysis highlighted that caproate was positively correlated with two genera (*Faecalibacterium* and *Allisonella*) and four differentially expressed genes (*ZNF134*, *TBX5*, *NEU4* and *SEMA6D*), which were all significantly increased upon LDA exposure. Collectively, our study indicates that the growth-promoting effect of LDA exposure in early life is associated with the shifts of colonic microbiota to increase utilization of carbohydrates and energy, enhanced SCFAs production and colonic functions.

1. Introduction

Previous studies have showed that the exposure of antibiotics in prepubertal children may lead to overweight, obesity or diabetes [1–3]. Although the altered microbiota and metabolism in childhood have been proposed to play a causal role in overweight and metabolic diseases, such as obesity and diabetes in later life [4–7], the underlying mechanism is still limited. Gut microbiota is involved in the digestion of proteins, lipids and carbohydrates in small intestine, and fermenting indigestible polysaccharides into low-molecular-weight metabolites, *e.g.* short-chain fatty acids (SCFAs) in large intestine. Particularly, SCFAs represent 10% of the human daily energy intake [8] and modulate crucial biological process, such as hepatic gluconeogenesis [9] and cholesterol biosynthesis [10–12] et al. Although metagenomic approaches have facilitated characterization of bacteria responsible for SCFAs production [13], studies addressing the link between gut microbiota and SCFAs and their role in host metabolism and growth are still limited.

The sub-therapeutic use of antibiotics in animal feed has been widely shown to promote feed intake and rapid growth [14]. Pigs possess similar structure and physiology of gastrointestinal tract [15], as well as microbiome as human beings [16], representing a good animal model for studying host interaction with gut microbiota in response to antibiotics. In this study, therefore, weaned piglets fed with or without antibiotics were employed to determine growth phenotypes, gut microbiota, SCFAs and colonic transcriptomes, further correlation and co-occurrence analysis were conducted across microbiota, SCFAs and gene expressions.

2. Materials and methods

2.1. Animals and diets

The study was approved by the Sichuan Agricultural University animal welfare committee and carried out in accordance with the National Research Council's Guide for the Care and Use of Laboratory Animals. Twenty-eight female piglets with body weight

* Correspondence to: L. Che, Animal Nutrition Institute, Sichuan Agricultural University, Ya'an 625014, Sichuan, China. Tel.: +86 13982285213; fax: +86 28 86290922.
E-mail addresses: clianqiang@hotmail.com (L. Che), flys828@gmail.com (F. Gao).
[1] These authors contributed equally to this work.

https://doi.org/10.1016/j.jnutbio.2019.108246

at 6.50±0.20 kg were weaned at 21 day-old-age, and randomly divided into two groups, receiving basic diet (n=14) and diet supplemented with LDA (n=14), respectively. LDA group was applied by adding the premix of chlortetracycline (10% purity) and virginiamycin (50% purity) at 750 mg/kg and 50 mg/kg diet, respectively. The dietary formulation was indicated in Supplementary file 1: Table S1.

Throughout the study, the feed supplied to the piglets were recorded daily. Individual piglet BW and feed disappearance was measured weekly to calculate average daily gain (ADG) and average daily feed intake (ADFI). For testing the digestibility of nutrients, during the third week, chromium oxide (Cr_2O_3) was added in each diet at 3 g/kg, a 4-d adaptation and 3-d collection of feces were conducted. The dry matter digestibility (DMD), energy digestibility (ED), crude protein digestibility (CPD) and crude fat digestibility (CFD) were determined and calculated as before [17]. Diarrhea score was recorded as our previous method [18]. After 28 days exposure of LDA, the contents of ileum and colon from piglets were obtained after euthanasia and flash frozen in liquid nitrogen. The weights of internal organs were recorded at dissection and relative weights of internal organs to body weights were calculated.

2.2. Targeted metabolomics of SCFAs detection

The concentrations of SCFAs, such as acetate, propionate, butyrate, valerate and caproate and short branched-chain fatty acids (SBCFAs), such as isobutyrate, 2-methyl butyrate, isovalerate and 4-methyl valerate were analyzed for the contents of both ileum and colon (Supplementary file 1: Table S2). The optimized UPLC-QTRAP-MS/MS method for more sensitive and accurate quantitation of SCFAs was employed in our study with some modifications [19]. With a single set of optimized reaction conditions, 3-nitrophenylhydrazine (3NPH) was employed for pre-analytical derivatization to convert SCFAs to their 3-nitrophenylhydrazones derivatives, which showed excellent in-solution chemical stability. Agilent 1100 UPLC system (Agilent, USA) coupled to a 4500 QTRAP triple-quadrupole mass spectrometer (AB Sciex, USA) equipped with the electrospray ionization (ESI) source was used for measuring SCFAs. The chromatographic separations were performed on a Waters BEH C18UPLC column (2.1×100 mm, 1.7 mm). The UPLC-MS/MS was operated in the negative-ion mode with a detection range of m/z 100–600. UPLC/MRM-MS data were acquired using the Analyst 1.5 software and processed using the MultiQuant 1.2 software (AB Sciex, USA). All the detailed experiment operations and parameters are shown Supplementary file 2.

2.3. Bacterial load by quantitative PCR (qPCR)

Total DNA was extracted from gut content for each sample using CTAB/SDS method. DNA was finally re-suspended in 50 μl DES (DNase/Pyrogen-Free Water) and measured by Qubit 3.0 Fluorometer. Each PCR reaction mixture (20 μl) contained 5 μl of template DNA, 10 μl SuperReal PreMix Plus (SYBR Green, TIANGEN, FP205), and 1.5 μl of each primer (10 μM; Forward: 5′-CCTACGGGAGGCAGCAG-3′; Reverse:5′-TTACCGCGGCTGCTGGCAC-3′). The qPCR reactions were performed in triplicate under thermal cycler conditions of 15 min at 95°C, and 39 cycles of 10 s at 95°C, 30 s at 55°C and 32 s at 72°C in a CFX Connect™ Real-Time PCR Detection System (BioRad). All results were normalized and calculated using the ΔCt method.

2.4. DNA extraction, PCR amplification of 16S rRNA gene, amplicon sequence and sequence data processing

Total genome DNA was extracted from contents of ileum and colon using CTAB/SDS method. DNA concentration measured by Qubit 3.0 Fluorometer and purity were monitored on 1% agarose gels. According to the concentration, DNA was diluted to 1 ng/μl using sterile water. 16S rRNA genes of distinct regions (V3-V4) were amplified used specific primer (357F-806R) with the barcode. All PCR reactions were carried out with Phusion High-Fidelity PCR Master Mix (New England Biolabs). Mix same volume of 1× loading buffer (contained SYB green) with PCR products and operate electrophoresis on 2% agarose gel for detection. Samples with bright main strip between 400–450 bp were chosen for further experiments. PCR products were mixed in equidensity ratios. Then, mixture PCR products were purified with Qiagen Gel Extraction Kit (Qiagen, Germany). Sequencing libraries were generated using TruSeq DNA PCR-Free Sample Preparation Kit (Illumina, USA) following manufacturer's recommendations and index codes were added. The library quality was assessed on the Qubit 2.0 Fluorometer (Thermo Scientific) and Agilent Bioanalyzer 2100 system. At last, the library was sequenced on an Illumina HiSeq2500 platform and 250 bp paired-end reads were generated.

2.5. 16S rRNA amplicon sequencing data analysis

Within QIIME2 (v2018.8) [20], sequences were quality-filtered and de-noised using the Divisive Amplicon Denoising Algorithm 2 (DADA2) [21]. Taxonomy was assigned using the 99% identity SILVA (release 119) V3-V4 classifier [22]. All the ribosomal sequence variants (RSVs) were identified as features across all samples without clustering. The feature table, rooted phylogenetic tree, representative sequences and metadata from QIIME2 were then exported for further analysis in R (v3.4.2). Shannon index and observed OTUs index were calculated with QIIME2 for Alpha diversity analysis, which presented complexity of species diversity for samples, and it was displayed with R. The difference tests of Alpha diversity for different groups were performed using Wilcoxon Rank Sum Test. Beta diversity was calculated using Bray-Curtis distance and Weighted UniFrac distance by the R package VEGAN (V2.5–3) [23], respectively. Differences in beta diversity were identified using Analysis of Similarity (ANOSIM) and effect size was indicated by an R-value (between −1 and + l, with a value of 0 representing the null hypothesis [24]), and PERMANOVA test leveraged by stress and effect size R^2 between 0 and 1. Community structure difference based on beta diversity was visualized using principal coordinate analysis (PCoA) by R package ape and non-metric multi-dimensional scaling (NMDS) method by R package VEGAN. Significantly different biomarkers at phylum and genus levels were identified using STAMP (v2.1.3) [25]. Significant correlations were indicated with an absolute Pearson's correlation coefficient above 0.50 and a P-value under 0.05. A self-developed Perl script was used to depict the links between genera and SCFAs with significant correlations. The co-occurrence networks were then visualized using Cytoscape 2.8.3. The PICRUSt was employed to predict community functional structure in our study [26], and the significantly different biomarkers including KEGG pathway and genes were identified by LEfSe [27], using selection criteria of alpha value for the factorial Kruskal-Wallis test of 0.05 and the linear discriminant analysis score of >2.5. The statistical significance for all analysis was set as P<.05.

2.6. RNA isolation, quantification, library preparation, sequencing and transcriptome analysis of intestinal tissues

Total RNAs of colon tissues were extracted by QIAGEN RNeasy Protect Animal Blood Kit (Qiagen, Germany). RNA degradation and contamination were monitored on 1% agarose gels. RNA purity was checked using the NanoPhotometer spectrophotometer (IMPLEN, CA, USA). RNA concentration was measured using Qubit RNA Assay Kit in Qubit 2.0 Flurometer (Life Technologies, CA, USA). RNA integrity was assessed using the RNA Nano 6000 Assay Kit of the Agilent Bioanalyzer 2100 system (Agilent Technologies, CA, USA). A total amount of 1.5 μg RNA per sample was used as input material for the RNA sample preparations. Sequencing libraries were generated using NEBNext UltraTM Directional RNA Library Prep Kit for Illumina (NEB, USA) following manufacturer's recommendations. Briefly, mRNA was purified from total RNA using poly-T oligo-attached magnetic beads. Fragmentation was carried out using divalent cations under elevated temperature in NEBNext First Strand Synthesis Reaction Buffer (5X). First strand cDNA was synthesized using random hexamer primer and M-MuLV Reverse Transcriptase (RNaseH-). Second strand cDNA synthesis was subsequently performed using DNA Polymerase I and RNase H. In the reaction buffer, dNTPs with dTTP were replaced by dUTP. Remaining overhangs were converted into blunt ends *via* exonuclease/polymerase activities. After adenylation of 3′ ends of DNA fragments, NEBNext Adaptor with hairpin loop structure were ligated to prepare for hybridization. In order to select cDNA fragments with right length, the library fragments were purified with AMPure XP system (Beckman Coulter, Beverly, USA). Then 3 μl USER Enzyme (NEB, USA) was used with size-selected, adaptor-ligated cDNA at 37°C for 15 min followed by 5 min at 95°C before PCR. Then PCR was performed with Phusion High-Fidelity DNA polymerase, Universal PCR primers and Index (X) Primer. At last, products were purified (AMPure XP system) and library quality was assessed on the Agilent Bioanalyzer 2100 system. From these libraries, 150-bp paired-end and strand-specific sequence reads were produced with Illumina HiSeq Xten. Tophat2 (v 2.1.0) was employed for performing read mapping to *Sus scrofa* genome reference (v11.1) [28]. The gene expression values were normalized by the number of metric fragments per kilobase of exon region per million mapped reads (FPKM) using Cufflinks (version 2.2.1) [29]. DEGs were obtained with an adjusted P-value cutoff $<=$ 0.05 and an absolute fold-change of $>=$ 2. GO enrichment of DEGs was performed using hypergeometric test according to *Sus scrofa* background and the results were visualized using GOplot package in R [30]. Multivariate Linear Fitting Model was employed to investigate the association among SCFAs, gut microbes and DEGs using R package lm. The formula in our model is as follows:

$$M \sim aS + bF + c$$

Where M is the concentration of SCFAs for all samples, S is the abundance of microbes for all samples, F is gene expression values of DEGs for all samples, a and b are coefficients, c is the intercept. The evaluation thresholds for models were adjusted R^2>= 0.8 and P<0.05.

2.7. Validation of DEG expression by real-time PCR

The total RNA was reversely transcribed by using PrimeScript RT reagent Kit with gDNA Eraser (Takara). Real-time PCR reaction mixture (10 μl) included fresh TB Green Premix Ex TaqII (5 μl), ROX Reference Dye II (0.2 μl), the primers (2 μl) and cDNA (2.8 μl). Real-time PCR reactions were performed as follows: one cycle (42°C 5 min); one cycle (95°C 10 s); forty cycles (95°C 5 s, 60°C 34 s); one cycle (95°C 15 s, 60°C 1 min and 95°C 15 s). The standard curve of each gene was run in duplicate and three times for obtaining reliable amplification efficiency values. The correlation coefficients (r) of all the standard curves were 0.99, and the amplification efficiency values were between 90 and 110%. All RT-PCR target gene expression was normalized to the expression of β-action and the relative quantification of gene expression was analyzed using the $2^{\Delta\Delta Ct}$ method. The sequences of primers, length of the products and GenBank accession were presented in Table S3.

3. Results

3.1. Growth performance and nutrients digestibility

After 4 weeks of treatment, the growth-promoting effect of LDA was observed, as indicated by the increased ADG (P=.026) and ADFI (P=.001). Meanwhile, the significantly increased nutrient digestibility such as DMD, ED, CPD and CFD (all P<.001), but decreased DS value (0.41 vs. 0.64, P<.001) were observed in the LDA group (Fig. 1a). In addition, the relative and absolute weights of kidney were increased in LDA groups (Supplementary file 3: Fig.S1).

3.2. SCFAs and SBCFAs

Regardless of LDA treatment, there were significantly higher (P<.001) levels of SCFAs and SBCFAs, such as acetate, propionate, isobutyrate, butyrate, isovalerate and valerate in the content of colon than in ileum (Supplementary file 3: Fig. S2). A principal component analysis (PCA) on both SCFAs and SBCFAs showed the considerable divergence between CON and LDA-treated piglets, regardless of intestinal sections (Fig. 1b). Particularly, the concentrations of SCFAs including caproate, 2-methyl butyrate and 4-methyl valerate were significantly increased in the LDA group relative to CON group (two-sided independent t-test P<.05, Fig. 1c).

3.3. Bacteria load and microbial diversity

To determinate the effect of LDA on the gut microbiota, the total bacterial load was analyzed by qPCR for both ileum and colon contents. The significantly higher quantity of bacterial load was revealed in the colon content than in the ileum content (Supplementary file 3: Fig.S3). Relative to CON group, the LDA group had significantly reduced total bacterial load in ileum content (2.59×10^{11} vs. 8.85×10^{11} 16S rRNA copies per gram), but not in colon contents (4.42×10^{13} vs. 4.23×10^{13} 16S rRNA copies per gram). We then employed SSU rRNA amplicon sequencing to analyze their microbial diversity. After quality-filtering, 7,287,313 high quality reads were acquired from 56 samples, enabling an average coverage of more than 0.12 million effective reads for each sample with a standard deviation of 6180 reads (Supplementary file 1: Table S4). A total of 4214 features were then identified according to DADA2 algorithm using QIIME2 (Supplementary file 1: Table S5). Alpha diversity analysis was performed for each group to compare the species diversity within each microbial community. As the Shannon index and observed OTUs index box plots showed, the diversity of bacterial OTUs in colon content was significantly greater (P<.001) than that in ileum content (Fig. 2a-b). However, no clear difference of alpha diversity was observed between the LDA and CON groups for either the colon or ileum content (Fig. 2a-b). Beta diversity analysis using both Nonmetric Multidimensional Scaling (NMDS) method, based on Bray-Curtis distance and Principal Coordinate Analysis (PCoA), as well as Weighted UniFrac distance of Features across samples, showing the significant shift of microbiota between ileum and colon contents (ANOSIM R=0.642, P=.001; PERMANOVA R^2=0.262, P=.001) (Fig. 2c-d). Similarly, beta diversity analysis showed the microbiota differences between colon and ileum content within group were more remarkable than that between LDA and CON group.

3.4. Bacterial abundance and functional implication

We examined the bacterial abundance at different taxonomic levels. The *Firmicutes* was the dominant phylum both in colon and ileum contents. However, the *Bacteroidetes* was dominant in colon, while *Proteobacteria* was dominant in ileum (Fig. 3a). At the genus level, most of the annotated features belonged to *Lachnospiraceae spp.*, *Lactobacillus, Ruminococcaceae_UCG-005, Ruminococcaceae_UCG-002* and *Clostridium_sensu_stricto_1* in colon, while the dominant genera were *Clostridium_sensu_stricto_1, Actinobacillus, Escherichia-Shigella, Turicibacter* and *Lactobacillus* in ileum (Supplementary file 3: Fig.S4). In the ileum content, the relative abundances at the genus level were less changed upon LDA exposure. The abundance of *Sarcina* was significantly decreased (P=.047), whereas the abundance of *Anaerovibrio* was increased (P=.038) in the ileum content of LDA group (Supplementary file 3: Fig.S5a). In contrast, the abundance of *Firmicutes* and *Actinobacteria* were significantly increased (P=.023 & P=.006, respectively), while the abundance of *Bacteroidetes* was decreased (P<.001) in the colon content of LDA group in comparison with CON group (Supplementary file 3: Fig. S5b). Consequently, the *Firmicutes*/*Bacteroidetes* value (F/B index) was significantly increased (P=.009) in colon content of LDA group (Fig. 3b). At the genus level, a total of 28 significantly different genera with average relative abundance >0.01% at least in one group was identified in the colon contents (Supplementary file 1: Table S6). Among these genera, 16 genera were significantly increased, while 12 genera were decreased (two-sided Welch's t-test P<.05) in the LDA group compared with CON group (Fig. 3c).

To further predict the functional changes of microbiota due to genera shifts upon LDA exposure, we then applied PICRUSt on our 16S rRNA data to compute the relative abundance of KEGG pathways. The enrichment of two level-2 KEGG pathways were significantly elevated upon LDA exposure (Fig. 3d, Supplementary file 3: Fig. S6a-b, Supplementary file 1: Table S7), including “carbohydrate metabolism” and “membrane transporters”. Among these pathways, the pathway of “membrane transporters” was comprised of three level-3 pathways (Supplementary file 1: Table S8), including the “phosphotransferase system (PTS)”, “ATP-binding cassette (ABC) transporters” and “transporters”. Among the 28 genera that were markedly changed in colon upon LDA exposure, the contribution degrees of *Collinsella, Blautia, Faecalibacterium, Phascolarctobacterium* and *Eubacterium* for the above pathways were profoundly improved (Fig. 3e).

3.5. Alteration of SCFAs production associates with gut microbiota shift

We further examined the correlation between microbiota abundance (Supplementary file 1: Table S9) and SCFAs production. As a result, the markedly changed SCFAs (2-methyl butyrate, 4-methyl valerate and caproate) in colon had significant correlations (absolute Pearson's coefficients >0.50 and P<.05) with the abundance of each genus (Fig. 4, Supplementary file 1: Tables S10/ S11). Both in the CoCA and CoCC group, all related genera (*Prevotella*_2, *Lachnospiraceae*_UCG-010, *Lachnospiraceae*_AC2044_group, *Methanobrevibacter*, et al.) were positively correlated with the three SCFAs. However, LDA exposure shifted the genera to highly correlate with the three SCFAs, as illustrated by the co-occurrence networks (Fig. 4). In the control group, the positively correlated genera were mainly comprised of *Prevotellaceae, Spirochaetaceae* and *Methanobacteriaceae*, whereas the genera of *Prevotellaceae* and *Spirochaetaceae* were not obviously correlated with those three SCFAs in the LDA group (Fig. 4b), probably due to their significant decrease of abundance upon LDA exposure. In contrast, the relative abundance of *Methanobrevibacter* was relatively increased upon LDA exposure (Fig. 4c) and the correlation between the *Methanobrevibacter* abundance and three SCFAs were strengthened from lowly positive to highly positive correlation (Fig. 4a-b). In addition, the positive correlation of *Ruminococcaceae* and *Lachnospiraceae genera* to SCFAs were strengthened upon LDA exposure, despite their abundances were not significantly changed. As indicated in the co-occurrence network (Fig. 4a-b), there were 11 genera positively correlating

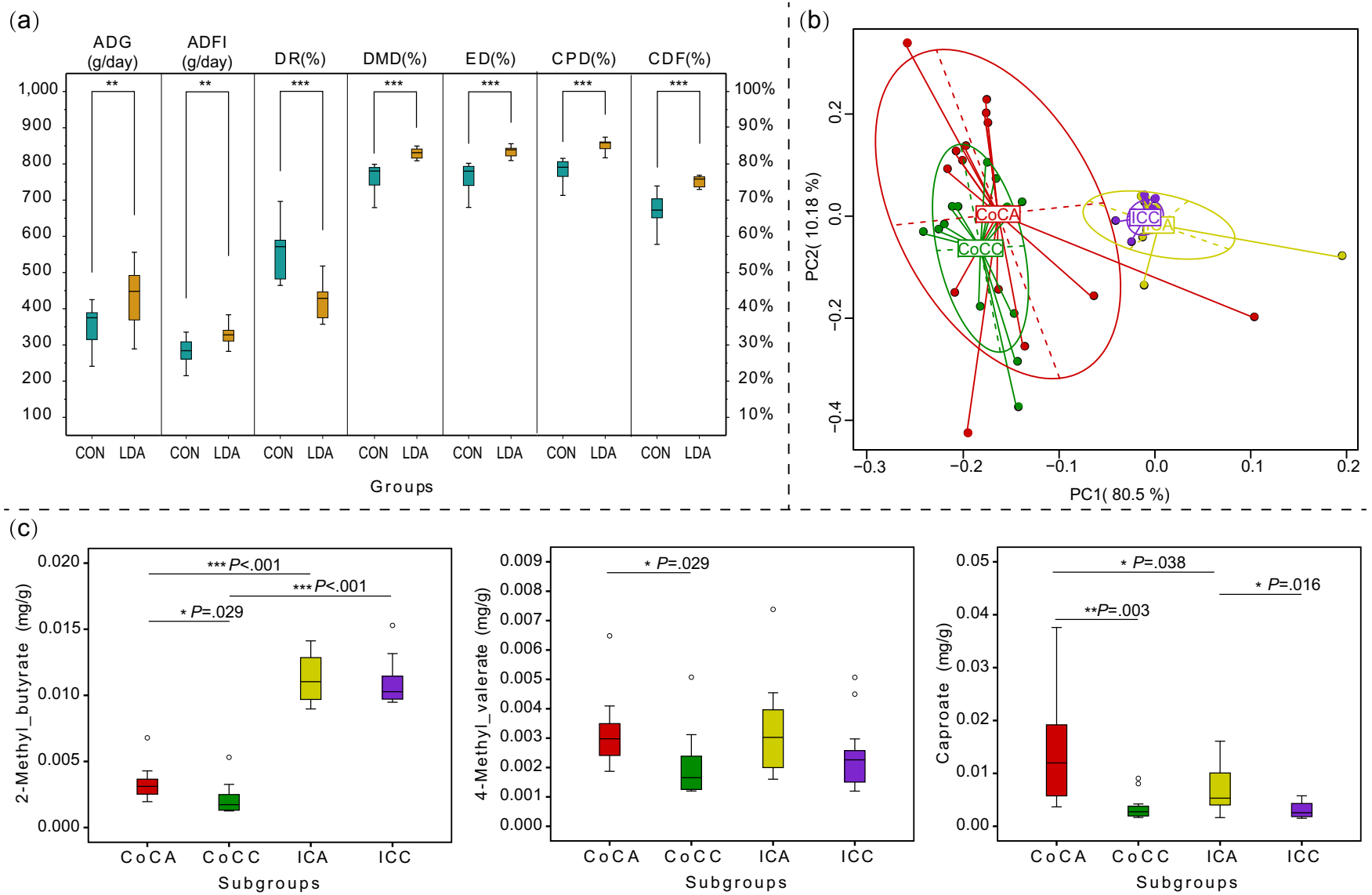

Fig. 1. The changes of host phenotype and SCFAs concentrations under LDA exposure. (a) The differential analysis of phenotype indexes using two-sided independent *t*-test method. ADG: average daily gain of body weight; ADFI: the average daily feed intake; DR: diarrhea rate; DMD: dry matter digestibility; ED: energy digestibility; CPD: crude protein digestibility; CFD: crude fatty digestibility. (b) Principal component analysis of four subgroups using all 9 SCFAs concentrations. (c) Boxplots showed the concentrations of three SCFAs (2-methyl butyrate, 4-methyl valerate and caproate) that were significantly different between LDA and CON groups either in the colon or the ileum contents. The *P* of two-sided independent t-test method was displayed, with<0.05 stands for statistical significance. One-asterisks stands for 0.01<*P*<.05 Double-asterisks stands for 0.001<*P*<.01, while triple asterisks stand for *P*<.001. CoCC: Colon content of CON group; CoCA: Colon content of LDA group; ICC: Ileum content of CON group; ICA: Ileum content of LDA group.

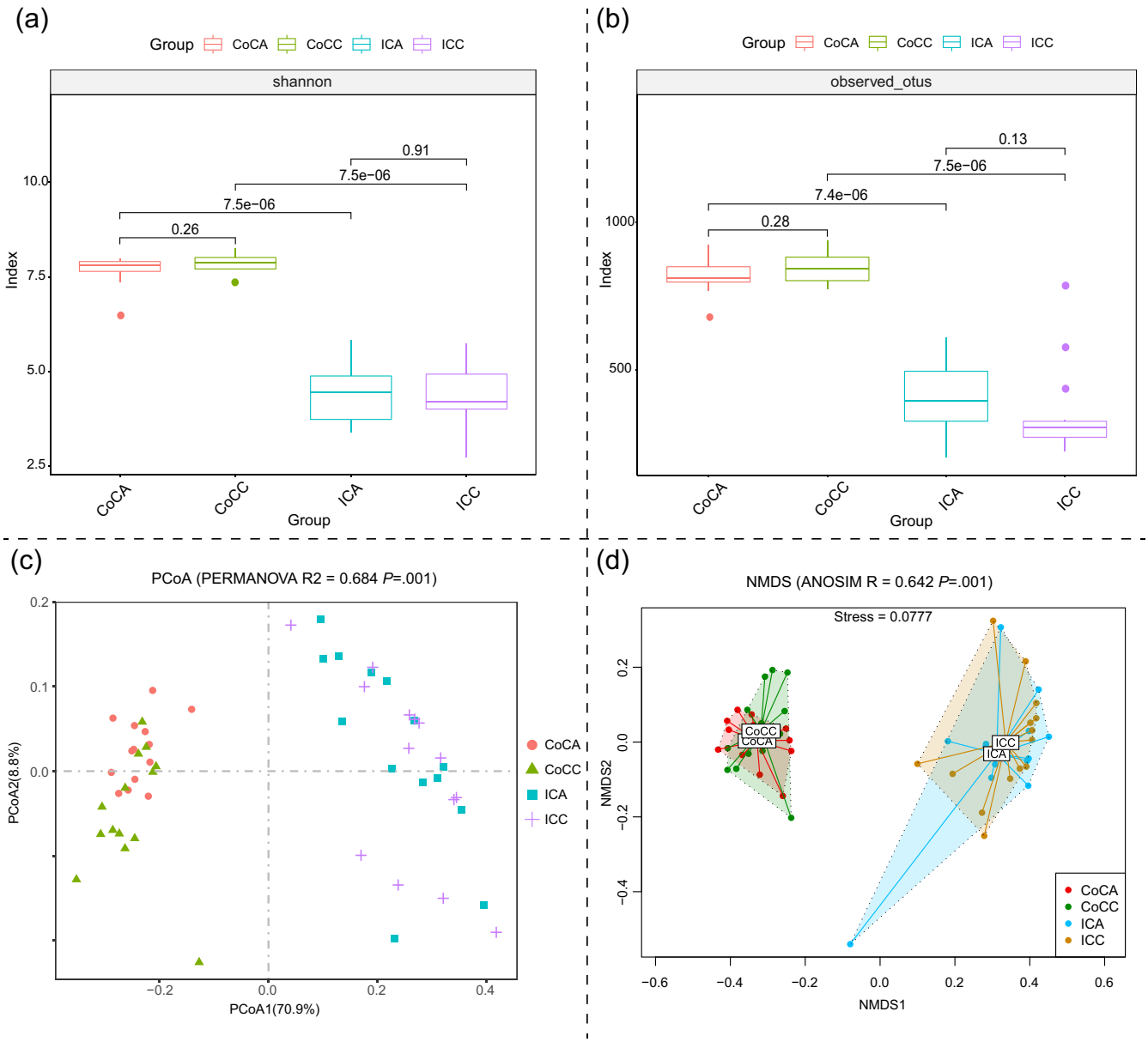

Fig. 2. Analysis of microbiota diversity in the ileum and colon contents between LDA and CON groups. (a) Alpha diversity analysis of all subgroups using Shannon index. (b) Alpha diversity analysis of all subgroups using observed OTUs index. (c) Beta diversity analysis of all subgroups using PCoA analysis based on Weighted UniFrac distance of Features. PERMANOVA test leveraged by stress and effect size R2 between 0 and 1. (d) Beta diversity analysis of all subgroups using NMDS analysis based on Bray-Curtis distance of Features. Analysis of Similarity (ANOSIM) and effect size was indicated by an R-value (between −1 and + l, with a value of 0 representing the null hypothesis). The numbers between groups in (a) and (b) mean P value. CoCC: Colon content of CON group; CoCA: Colon content of LDA group; ICC: Ileum content of CON group; ICA: Ileum content of LDA group.

with butyrate in LDA group, while only *Faecalibacterium, Butyricicoccus* and *Agathobacter* were positively correlating with butyrate in control group.

3.6. Gut microbiota shift and SCFAs alteration associate with colonic gene expressions

Considering the role of SCFAs on gene transcription, we further performed transcriptome analysis on the colonic tissues. We obtained 45.41±7.89 million clean reads per sample, of which 76.65±5.19% could be aligned to the pig reference genome (Supplementary file 1: Table S12). Fifty-two DEGs were identified (FC>2, *P*<.05), in which 49 were up-regulated upon LDA exposure (Supplementary file 1: Table S13). GO enrichment analysis indicated 16 DEGs were involved in biological process of “cell proliferation or normal development”, “immune response”, “nervous system”. (Supplementary file 1: Table S14, Fig. 5a). In the “cell proliferation” category, the transcriptions of all enriched genes were significantly up-regulated upon LDA exposure, including *FGF18*, *TBX5*, *NR6A1* and *NRG1* (Fig. 5b). Five genes were involved in the “immune response” category, including up-regulated gene expressions of *CXCL10, BPI, C6* and *MX1*, and down-regulated gene expressions of *CD200*. In addition, we found the up-regulated genes in relation with neuron cells, including *FGF14, NRG1, NTRK2* and *EFNA5* (Fig. 5b). Multivariate Linear Fitting Model analysis was further performed across SCFAs, gut microbes and DEGs. As a result, acetate, propionate, butyrate and caproate showed complex

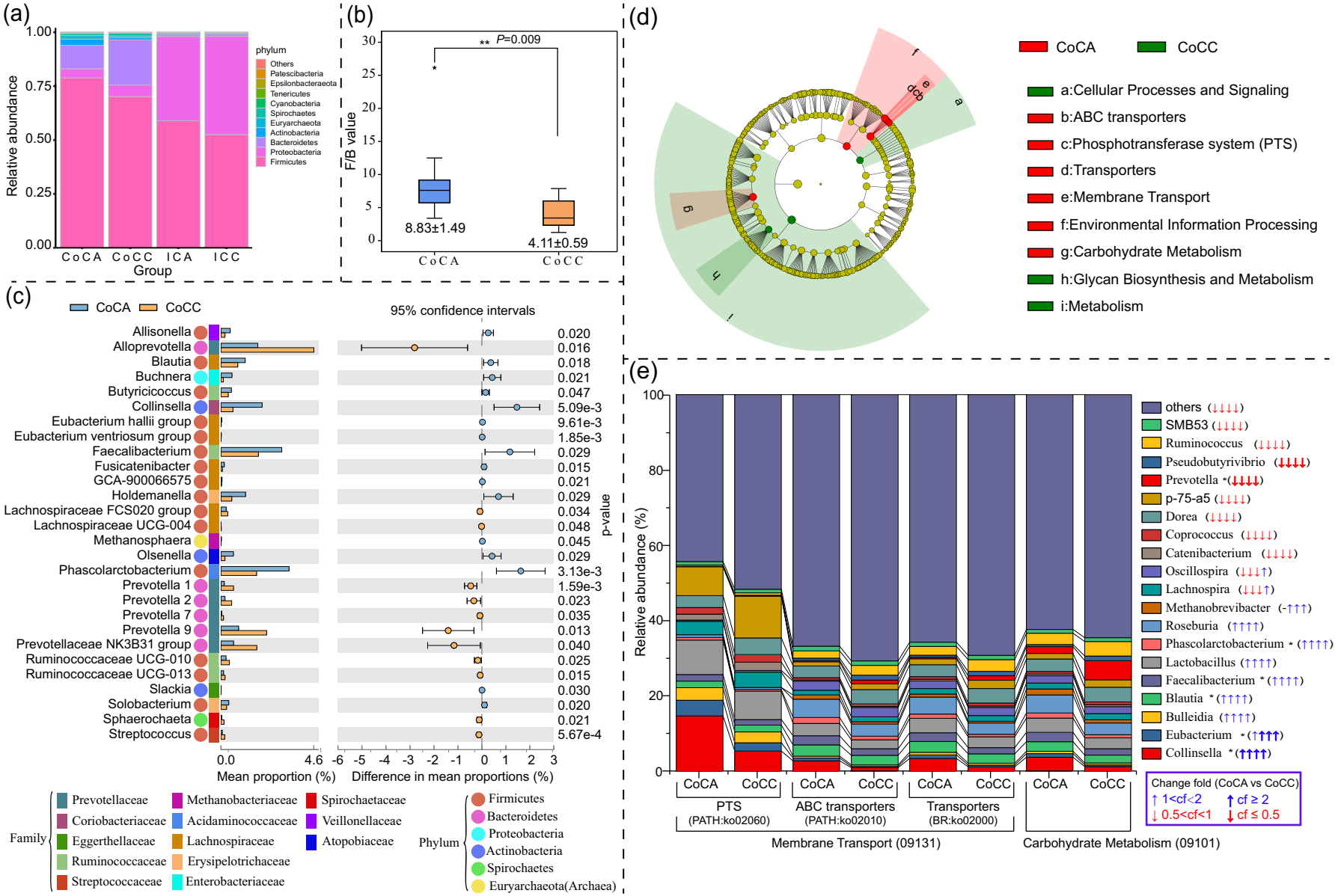

Fig. 3. LDA exposure altered the structure and function of the microbial community in colon content. (a) Stacked column chart on the relative abundance of microbial phylum in CoCC, CoCA, ICC and ICA subgroups. (b) *Firmicutes*/*Bacteroidetes* value (F/B index) between CoCC and CoCA subgroups. (c) Significantly different genera (two-sided Welch's *t*-test *P* of <0.05) in the colon content between LDA and CON groups, based on SILVA database annotation. (d) LEfSe analysis using the abundances of the PICRUSt-predicted KEGG orthologs (KO) functions. The significant pathways were selected based on both the Kruskal-Wallis test (alpha value <0.05) and the linear discriminant analysis score of greater than 2.5. (e) The stacked plot of relative abundance for contributing genera with functions enriched in the Phosphotransferase system (PTS), ABC transporters, Transporters and Carbohydrate Metabolism in the colon content for CoCC and CoCA subgroups. Double-asterisks stands for 0.001 < *P*<.01. CoCC: Colon content of CON group; CoCA: Colon content of LDA group.

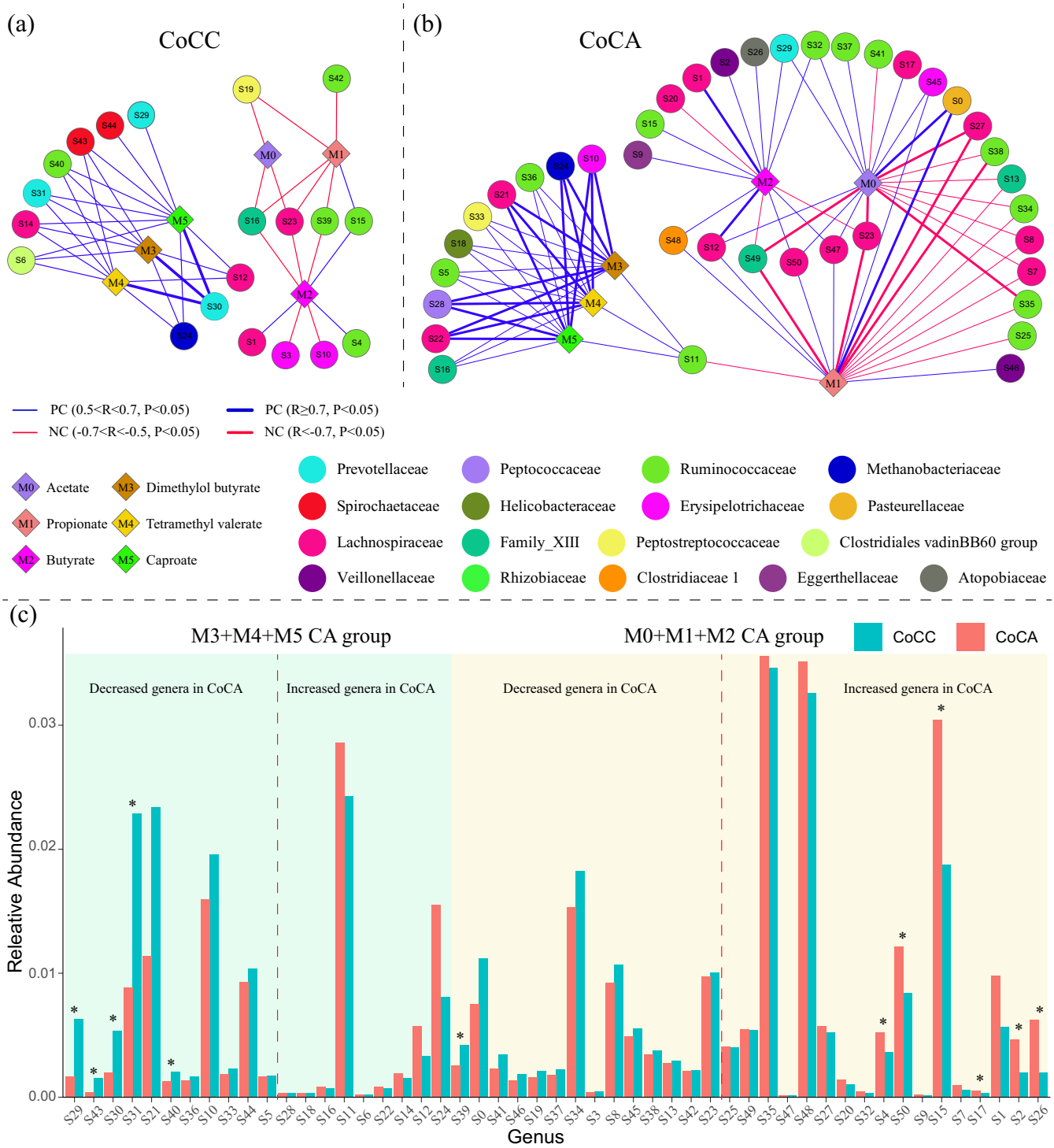

S0 Actinobacillus
S1 Agathobacter
S2 Allisonella
S3 Anaerorhabdus_furcosa_group
S4 Butyricicoccus
S5 Candidatus_Soleaferrea
S6 Clostridiales_vadinBB60_group_uncultured_bacterium
S7 Coprococcus_2
S8 Coprococcus_3
S9 Enterorhabdus
S10 Erysipelotrichaceae_uncultured
S11 Eubacterium_coprostanoligenes_group
S12 Eubacterium_eligens_group
S13 Eubacterium_nodatum_group
S14 Eubacterium_xylanophilum_group
S15 Faecalibacterium
S16 Family_XIII sp.
S17 GCA-900066575
S18 Helicobacter
S19 Intestinibacter
S20 Lachnoclostridium
S21 Lachnospiraceae_AC2044_group
S22 Lachnospiraceae_UCG-010
S23 Lachnospiraceae_XPB1014_group
S24 Methanobrevibacter
S25 Negativibacillus
S26 Olsenella
S27 Oribacterium
S28 Peptococcaceae_uncultured
S29 Prevotella_1
S30 Prevotella_2
S31 Prevotella_9
S32 Pygmaiobacter
S33 Romboutsia
S34 Ruminococcaceae_NK4A214_group
S35 Ruminococcaceae_UCG-002
S36 Ruminococcaceae_UCG-004
S37 Ruminococcaceae_UCG-008
S38 Ruminococcaceae_UCG-009
S39 Ruminococcaceae_UCG-010
S40 Ruminococcaceae_UCG-013
S41 Ruminococcaceae_uncultured
S42 Ruminococcus_2
S43 Sphaerochaeta
S44 Treponema_2
S45 Turicibacter
S46 Veillonella
S47 Pseudochrobactrum
S48 Clostridium_sensu_stricto_1
S49 Family_XIII_AD3011_group
S50 Blautia

Fig. 4. LDA exposure changed main contributors to the production of 2-methyl butyrate, 4-methyl valerate, caproate, acetate, propionate and butyrate in the colon content. (a) Co-occurrence network analysis between microbe genera and the SCFAs for the colon contents without LDA exposure. (b) Co-occurrence network analysis between microbe genera and the

correlation networks with DEGs and gut microbes (Fig. 5c). Especially, caproate was positively correlated with two genera (*Faecalibacterium* and *Allisonella*) and 4 DEGs (*ZNF134*, *TBX5*, *NEU4* and *SEMA6D*), which were all significantly increased upon LDA exposure (Fig. 5c). A qPCR validation was then performed on the expression of 9 DEGs that also displayed significant correlation with the changed SCFAs and genera (Supplementary file 1: Table S15). Two genes (*ZNF134 and NR6A1*) were confirmed with significant up-regulation ($P<.05$), while the rest genes also showed the same tendency of increased expression upon antibiotics exposure (Supplementary file 1: Table S16).

4. Discussion

The early exposure to antibiotics has been shown to increase risk of overweight or obesity later in childhood [3,31,32], but the causal role of this exposure is not clear. We proposed that the changing intestinal microbiota by antibiotics may influence intestinal function and host metabolism and the related phenotypes. The growth-promoting effect of LDA in pig model mimics the similar consequences in human-being, in which infants grow faster with increasing risks of overweight or obesity when receiving antibiotics treatment in early life [33]. In this study, we did find the sub-therapeutic use of antibiotics markedly increased the food intake and growth rate of pigs. Furthermore, we found LDA markedly decreased the total bacterial load in ileum but not in colon, probably due to that the total bacterial load in the colon content is much higher than in the ileum content and LDA was not sufficient to change the absolute numbers of bacterial cells. Despite of that, although the bacterial load of ileum content was significantly reduced, neither SCFA production nor ileum gene expression (data not shown) was affected. In contrast, the altered structure of the colonic microbiota is associated with changes of the SCFA production and colonic gene expression. These results highlighted the significance of colon as a major organ for the nutritional effects of microbiota, as indicated by the markedly increased F/B index and the members of the *Firmicutes* and *Actinobacteria phyla* include species degrading the dietary carbohydrates [34,35]. Likewise, the increased *Methanosphaera species* in colon upon LDA exposure has been associated with obesity [36] and host energy extraction from indigestible polysaccharides [37], explaining the higher digestibility of DM in this study.

In addition, the increased abundances of *Blautia, Collinsella, Eubacterium, Faecalibacterium* and *Phascolarctobacterium* in colon upon LDA exposure enhanced pathways such as "carbohydrate metabolism", "phosphotransferase system (PTS)" and "ATP-binding cassette transporters", based on the PICRUSt prediction on functional changes. PTS is related to the uptake and phosphorylation of multiform carbohydrates and involved in microbial degradation of carbohydrates in *Firmicutes* and *Actinobacteria*, enhancing cells to import simple sugars over carbohydrates [38]. Meanwhile, the ATP-binding cassette transporters were suggested to increase the transport of lipids and be overrepresented in obese children. These results implied LDA exposure induced the functional changes of microbiota for improving carbohydrates utilization and energy metabolism, and being beneficial for host growth. In addition, the role of gut microbiota in influencing host food intake has been proposed [39], in this study, the increased food intake by LDA exposure may be also related to the changing microbiota, particularly the decreased abundance of *Prevotellaceae* upon LDA exposure has been shown to negatively correlate with ghrelin [40], a GIT neuropeptide acting on hypothalamic brain cells to increase appetite, gastric acid secretion and gastrointestinal motility [41].

As key bacterial metabolites by gut bacteria, SCFAs play crucial role in linking microbiota composition and various biological effects [12]. The quantitative correlation between microbiota abundance and SCFAs levels revealed the stronger correlation of *Ruminococcaceae, Lachnospiraceae* and *Methanobrevibacter*, less correlation of *Prevotella 9, Prevotella 2, Prevotella 1* and *Sphaerochaeta* with 2-methyl butyrate, 4-methyl valerate and caproate, which were significantly increased in the colon content of piglets upon LDA exposure. The members of *Ruminococcaceae* are associated with fermenting indigestible polysaccharides into SCFAs, the increase in these taxa leaded to more calorie uptake through increasing the availability of SCFAs [40]. In addition, LDA exposure shifted more genera to be positively correlated to acetate, propionate and butyrate, including *Faecalibacterium, Lachnospiraceae group* and *Clostridium* that are well-known SCFAs producing bacteria belonging to the *Firmicutes phylum* [42–44]. Therefore, the microbial community in colon contributing to SCFAs production was enriched upon LDA exposure.

Considering the crucial role of SCFAs in gut health and immunology [45,46], we further performed Multivariate Linear Fitting Model analysis among the altered SCFAs, gut microbiota and DEGs. Caproate, as one of the SCFAs in reducing pathogenic colonization in the gut [47], showed a complex correlation network with DEGs and gut microbiota. LDA exposure significantly up-regulated the immunity-related expressions of genes such as *CXCL10, BPI, C6* and *MX1* for the host immunity [48,49] and antiviral effect [50,51], also genes (*FGF14, FGF18, NRG1, TBX5, NR6A1, NTRK2* and *EFNA5*) related to cell proliferation and nervous development. These results on transcription alteration indicate the LDA exposure influences the gut signaling and function, which could be ascribed to the shifting of microbiota structure and changes of fermentation metabolites in the colon caused by LDA, interacting with local tissue and cell functions.

In summary, the growth-promoting effect of LDA exposure in early life could be related to the increasing food intake and digestibility of nutrients, which are associated with microbiota shifts for SCFA production and better energy utilization, as well as host–microbe interactions. These findings reveal the potential mechanism on the risk of childhood overweight caused by antibiotic exposure in early life.

Acknowledgements

This work is funded by Central Public-interest Scientific Institution Basal Research Fund (No. Y2017JC26), the Agricultural Science and Technology Innovation Program Cooperation and Innovation Mission (CAAS-XTCX2016), Fundamental Research Funds for Central Non-profit Scientific Institution (No. Y2017JC26) and the National Key Research and Development Program of China (grant number 2016YFD0501204).

Data Availability Statements

The datasets generated and analyzed during the current study are available in the NCBI Sequence Read Archive (SRA) repository. The 16S

SCFAs for the colon contents with LDA exposure. Circle nodes represent microbe genera and diamond nodes denote SCFAs. Each co-occurring pair between genus and SCFAs had an absolute Pearson correlation above 0.50 [blue thin line indicates general positive correlation ($0.5<R<0.70$); blue thick line indicates strong positive correlation ($R>0.70$); red thin line indicates general negative correlation ($-0.7 < R<-0.50$)] with a significance level under 0.05. Circles with distinct color represent the genera from the different families. Edge lines with distinct color are in direct proportion to the direction of correlation (red means negative correlation-NC; blue means positive correlation-PC). The width of edge line represents the strength of correlation. (c) The relative abundances of related genera between CoCC and CoCA. Asterisk stands for statistical significance ($P<.05$). CoCC: Colon content of CON group; CoCA: Colon content of LDA group.

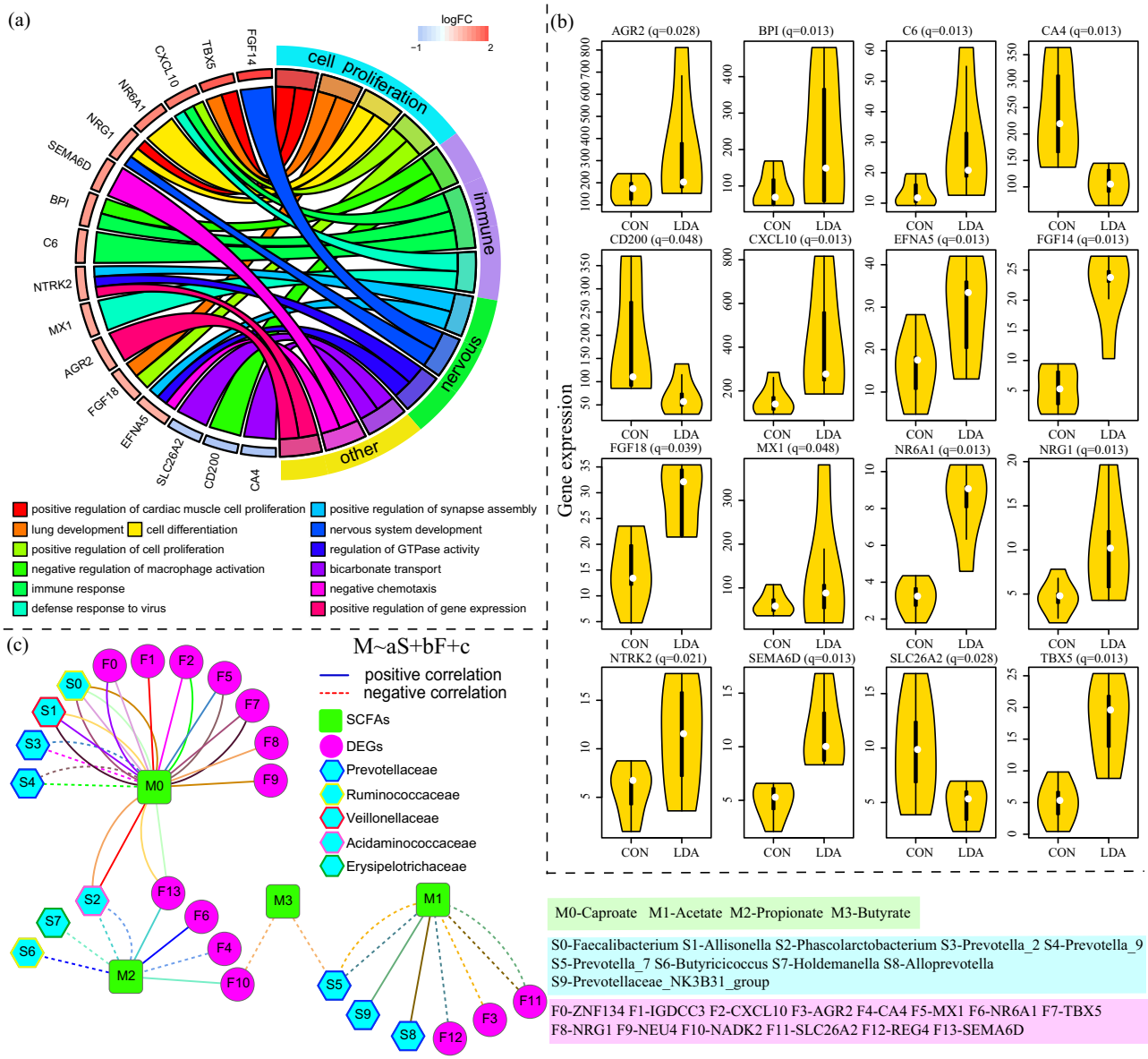

Fig. 5. Go enrichment of DEGs and correlation analysis between SCFAs and DEGs. (a) GOChord plot displays the relationship between a list of BP terms and corresponding genes. The DEGs located in plot left were ordered according to their logFC. The GO terms located in plot right were cluster as server category, including cell proliferation, immune, nervous and others. (b) The gene expression violin box plots of 16 DEGs, which present in enriched GO terms. The white points depict median values, the black boxes connect the 25th and 75th percentiles and the thin black lines connect the lower adjacent value to the upper adjacent value. The yellow area depicts a density trace, plotted symmetrically above and below the horizontal box plot. Two-sided independent t-test was used to identify significant differences of gene expression levels between each pair. (c) Multivariate Linear Fitting Model analysis the altered SCFAs, significant different gut microbes and gene expression of all these DEGs. Circle nodes represent DEGs, hexagon nodes mean genera and round rectangle nodes denote SCFAs. Each model among gene, microbe and SCFAs had the same color connection lines. (Full lines indicate general positive correlation; dotted lines indicate negative correlation.)

rRNA amplicon data is linked to SRP118553, accession numbers SRR6058541, SRR6058555, SRR6058585-SRR6058593, SRR6058597, SRR6058602-SRR6058603, SRR6058605-SRR6058608, SRR6058610, SRR6058624, SRR6058626, SRR6058628, SRR6058631-SRR6058639, SRR6058641-SRR6058646, SRR6058653- SRR6058671. The strand-specific RNA-seq data is linked to accession numbers SRR6746572 -SRR6746582.

Declarations

Ethics approval and consent to participate

All animal work of this study was approved by the Sichuan Agricultural University animal welfare committee and carried out in accordance with the National Research Council's Guide for the Care and Use of Laboratory Animals.

Authors' contributions

FG, LC, DC, DW and QH designed the study; RW, ZF, YL, SX and BF collected samples and performed animal experiments; CL performed qPCR experiment; QH, DZ, YZ, RW and GX processed and analyzed data; QH, FG and LC interpreted data and wrote the manuscript. All authors approved the final manuscript.

Competing interests

The authors declare that they have no competing interests.

Appendix A. Supplementary data

The Supplementary material for this article can be found at the Journal of Nutritional Biochemistry website. Supplementary data to this article can be found online at https://doi.org/10.1016/j.jnutbio.2019.108246.

References

[1] Scott FI, Horton DB, Mamtani R, Haynes K, Goldberg DS, Lee DY, et al. Administration of Antibiotics to Children Before Age 2 Years Increases Risk for Childhood Obesity Gastroenterology, 151 (2016), pp. 120–129 e125.
[2] Saari A, Virta LJ, Sankilampi U, Dunkel L, Saxen H. Antibiotic exposure in infancy and risk of being overweight in the first 24 months of life. Pediatrics 2015;135:617–26.
[3] Bailey LC, Forrest CB, Zhang P, Richards TM, Livshits A. DeRusso PA. Association of antibiotics in infancy with early childhood obesity JAMA Pediatr 2014;168:1063–9.
[4] Boulange CL, Neves AL, Chilloux J, Nicholson JK, Dumas ME. Impact of the gut microbiota on inflammation, obesity, and metabolic disease. Genome Med 2016;8:42.
[5] Moreno-Indias I, Cardona F, Tinahones FJ. Queipo-Ortuno MI. Impact of the gut microbiota on the development of obesity and type 2 diabetes mellitus Front Microbiol 2014;5:190.
[6] Torres-Fuentes C, Schellekens H, Dinan TG. Cryan JF. The microbiota–gut–brain axis in obesity The Lancet Gastroenterology & Hepatology 2017;2:747–56.
[7] Abdelaal M, le Roux CW, Docherty NG. Morbidity and mortality associated with obesity Ann Transl Med, 5 (2017), pp. 161.
[8] Samuel BS. Gordon JI. A humanized gnotobiotic mouse model of host-archaeal-bacterial mutualism Proc Natl Acad Sci U S A 2006;103:10011–6.
[9] Xie C, Jiang C, Shi J, Gao X, Sun D. Sun L, et al. An intestinal farnesoid X receptorcCeramide signaling axis modulates hepatic gluconeogenesis in mice diabetes 2017;66:613–26.
[10] Caesar R, Nygren H, Oresic M, Backhed F. Interaction between dietary lipids and gut microbiota regulates hepatic cholesterol metabolism. J Lipid Res 2016;57:474–81.
[11] Richards JL, Yap YA, McLeod KH, Mackay CR. Mariño E. Dietary metabolites and the gut microbiota: an alternative approach to control inflammatory and autoimmune diseases Clinical & Translational Immunology 2016;5:e82.
[12] Koh A, De Vadder F, Kovatcheva-Datchary P, Backhed F. From dietary fiber to host physiology: short-chain fatty acids as key bacterial metabolites cell, 165 (2016), pp. 1332–1345.
[13] Morrison DJ. Preston T. Formation of short chain fatty acids by the gut microbiota and their impact on human metabolism gut microbes 2016;7:189–200.
[14] Graham J, Boland J. Silbergeld E. Growth promoting antibiotics in food animal production: an economic analysis public health reports 2007;122:79–87.
[15] Sangild PT. Gut responses to enteral nutrition in preterm infants and animals Exp biol med (Maywood), 231 (2006), pp; 1695-1711.
[16] Xiao L, Estelle J, Kiilerich P, Ramayo-Caldas Y, Xia Z. Feng Q, et al. A reference gene catalogue of the pig gut microbiome Nat Microbiol 2016;1:16161.
[17] Favero A, Ragland D, Vieira SL, Owusu-Asiedu A, Adeola O. Digestibility marker and ileal amino acid digestibility in phytase-supplemented soybean or canola meals for growing pigs. J Anim Sci 2014;92:5583–92.
[18] Wang Y, Kuang Y, Zhang Y, Song Y, Zhang X, Lin Y, et al. Rearing conditions affected responses of weaned pigs to organic acids showing a positive effect on digestibility, microflora and immunity Anim Sci J 2016;87:1267–80.
[19] Han J, Lin K, Sequeira C. Borchers CH. An isotope-labeled chemical derivatization method for the quantitation of short-chain fatty acids in human feces by liquid chromatography–tandem mass spectrometry Analytica Chimica Acta 2015;854:86–94.
[20] Bolyen E, Rideout JR, Dillon MR, Bokulich NA, Abnet C, Al-Ghalith GA, et al. QIIME 2: Reproducible, interactive, scalable, and extensible microbiome data science PeerJ Preprints, 6 (2018), pp. e27295v27292.
[21] Callahan BJ, McMurdie PJ, Rosen MJ, Han AW, Johnson AJ, Holmes SP. DADA2: high-resolution sample inference from Illumina amplicon data. Nat Methods 2016;13:581–3.
[22] Quast C, Pruesse E, Yilmaz P, Gerken J, Schweer T. Yarza P, et al. The SILVA ribosomal RNA gene database project: improved data processing and web-based tools Nucleic Acids Research 2012;41:D590–6.
[23] Oksanen J, Blanchet FG, Kindt R, Legendre P, Minchin PR, O'hara R, et al. Package 'vegan' Community ecology package, version, 2 (2015).
[24] Clarke KR. Non-parametric multivariate analyses of changes in community structure. Australian journal of ecology 1993;18:117–43.
[25] Parks DH, Tyson GW, Hugenholtz P. Beiko RG. STAMP: statistical analysis of taxonomic and functional profiles Bioinformatics 2014;30:3123–4.
[26] Langille MGI, Zaneveld J, Caporaso JG, McDonald D, Knights D, Reyes JA, et al. Predictive functional profiling of microbial communities using 16S rRNA marker gene sequences Nature Biotechnology 2013;31:814–21.
[27] Segata N, Izard J, Waldron L, Gevers D. Miropolsky L. Metagenomic biomarker discovery and explanation genome biology 2011;12:R60.
[28] Kim D, Pertea G, Trapnell C, Pimentel H, Kelley R, Salzberg SL. TopHat2: accurate alignment of transcriptomes in the presence of insertions, deletions and gene fusions. Genome Biol 2012;14:R36.
[29] Trapnell C, Williams BA, Pertea G, Mortazavi A, Kwan G. Baren MJV, et al. Transcript assembly and quantification by RNA-Seq reveals unannotated transcripts and isoform switching during cell differentiation Nature Biotechnology 2010;28:511–5.
[30] Walter W, Sanchez-Cabo F. Ricote M. GOplot: an R package for visually combining expression data with functional analysis bioinformatics 2015;31:2912–4.
[31] Fetissov SO. Role of the gut microbiota in host appetite control: bacterial growth to animal feeding behaviour Nat Rev Endocrinol 2017;13:11–25.
[32] Turta O, Rautava S. Antibiotics, obesity and the link to microbes — what are we doing to our children? BMC Med 2016;14:57.
[33] Rasmussen SH, Shrestha S, Bjerregaard LG, Angquist LH, Baker JL. Jess T, et al. Antibiotic exposure in early life and childhood overweight and obesity: A systematic review and meta-analysis Diabetes Obes Metab 2018;20:1508–14.
[34] Flint HJ, Scott KP, Duncan SH, Louis P. Forano E. Microbial degradation of complex carbohydrates in the gut Gut microbes 2012;3:289–306.
[35] Leitch EC, Walker AW, Duncan SH, Holtrop G. Flint HJ. Selective colonization of insoluble substrates by human faecal bacteria Environ Microbiol 2007;9:667–79.
[36] Zhanga H, DiBaiseb JK, Zuccoloc A, Kudrnac D, Braidottic M. Yuc Y, et al. Human gut microbiota in obesity and after gastric bypass Proceedings of the National Academy of Sciences 2009;106:2365–70.
[37] Zhang H, Dibaise JK, Zuccolo A, Kudrna D, Braidotti M. Yu Y, et al. Human gut microbiota in obesity and after gastric bypass Proc Natl Acad Sci U S A 2009;106:2365–70.
[38] Turnbaugh PJ, Backhed F, Fulton L. Gordon JI. Diet-induced obesity is linked to marked but reversible alterations in the mouse distal gut microbiome Cell Host Microbe 2008;3:213–23.
[39] Ridaura VK, Faith JJ, Rey FE, Cheng J, Duncan AE. Kau AL, et al. Gut Microbiota from Twins Discordant for Obesity Modulate Metabolism in Mice Science 2013;341:1241214.
[40] Gomez-Arango LF, Barrett HL, McIntyre HD, Callaway LK, Morrison M. Nitert MD. Connections Between the Gut Microbiome and Metabolic Hormones in Early Pregnancy in Overweight and Obese Women DIABETES 2016;65:2214–23.
[41] Schwartz MW, Woods SC, Porte D, Seeley RJ. Baskin DG. Central nervous system control of food intake NATURE 2000;404:661–71.
[42] Duncan SH, Holtrop G, Lobley GE, Calder AG, Stewart CS. Flint HJ. Contribution of acetate to butyrate formation by human faecal bacteria Br J Nutr 2004;91:915–23.
[43] Meehan CJ, Beiko RG. A Phylogenomic View of Ecological Specialization in the Lachnospiraceae, a Family of Digestive Tract-Associated Bacteria Genome Biology and Evolution 2014;6:703–13.
[44] Zhang J, Guo Z, Xue Z, Sun Z, Zhang M, Wang L, et al. A phylo-functional core of gut microbiota in healthy young Chinese cohorts across lifestyles, geography and ethnicities ISME J 2015;9:1979–90.
[45] Donohoe DR, Garge N, Zhang X, Sun W, O'Connell TM. Bunger MK, et al. The Microbiome and Butyrate Regulate Energy Metabolism and Autophagy in the Mammalian Colon CELL METABOLISM 2011;13:517–26.
[46] Guilloteau P, Martin L, Eeckhaut V, Ducatelle R, Zabielski R. Van Immerseel F. From the gut to the peripheral tissues: the multiple effects of butyrate Nutrition Research Reviews 2010;23:366–84.
[47] Van Immerseel F, De Buck J, Boyen F, Bohez L, Pasmans F, Volf J, et al. Medium-chain fatty acids decrease colonization and invasion through hilA suppression shortly after infection of chickens with *Salmonella enterica* serovar Enteritidis Appl Environ Microbiol 2004;70:3582–7.
[48] Spicer ST, Tran GT, Killingsworth MC, Carter N, Power DA, Paizis K, et al. Induction of passive Heymann nephritis in complement component 6-deficient PVG rats Journal of Immunology 2007;179:172.
[49] Akin H, Tahan G, Ture F, Eren F, Atug O, Tahan V, et al. Association between bactericidal/permeability increasing protein (BPI) gene polymorphism (Lys216-Glu) and inflammatory bowel disease J Crohns Colitis 2011;5:14–8.
[50] Dufour JH, Dziejman M, Liu MT, Leung JH, Lane TE, Luster AD. IFN-gamma-inducible protein 10 (IP-10; CXCL10)-deficient mice reveal a role for IP-10 in effector T cell generation and trafficking. J Immunol 2002;168:3195.
[51] Haller O, Staeheli P. Kochs G. Interferon-induced Mx proteins in antiviral host defense Biochimie 2007;89:812.